IJE TRANSACTIONS C: Aspects Vol. 36 No. 06, (June 2023) 1099-1113

International Journal of Engineering

Journal Homepage: www.ije.ir

Irradiation and Temperature Estimation with a New Extended Kalman Particle Filter for Maximum Power Point Tracking in Photovoltaic Systems

M. Hooshmand, H. Yaghobi*, M. Jazaeri

Faculty of Electrical and Computer Engineering, Semnan University, Semnan, Iran

PAPER INFO

Paper history:
Received 14 February 2023
Received in revised form 29 March 2023
Accepted 30 March 2023

Keywords:
Photovoltaic Systems
Maximum Power Point Tracking Particle Filter
Extended Kalman Filter
Estimation

ABSTRACT

In this paper, a new method, based on the estimation of irradiation and temperature values, was proposed for Maximum Power Point Tracking (MPPT) in photovoltaic systems. The proposed estimation method is based on a new Extended Kalman Particle Filter (EKPF). Given that the basis of the proposed method is a particle filter, firstly, the estimation is performed with high accuracy, although the target system has severe nonlinearity; secondly, there is no limitation for the probability density functions of the measurement and process noise. This method works for Gaussian and non-Gaussian noises. To show the estimation accuracy, the proposed method will be compared with the common method based on extended Kalman filter (EKF) and both methods will be evaluated due to the root means square error criterion. Due to the accurate estimation, MPPT is performed with good performance. For validation, the proposed MPPT method was compared with the EKF method and the conventional incremental conductance (InC) method. The simulations show that the efficiency is improved from 0.1% to 1% compared to the EKF, and from 0.8% to 8.65% compared to the InC method, which shows the performance of the proposed MPPT method in noisy environments.

doi: *10.5829/ije.2023.36.06c.08*

1. INTRODUCTION

Increasing demand for electricity and increasing attention paid to the environmental impacts of the conventional electricity generation, have led the world to focus on using renewable energy sources such as fuel cells, wind power, and photovoltaic systems. Due to the many advantages of photovoltaic (PV) systems, the demand for electricity generation by them, both on-grid and off-grid, is increasing [1, 2]. The power generated in a PV module depends on the amount of irradiation and its temperature. Therefore, with changing weather conditions, the output power changes [3]. The I-V characteristic of PV modules is nonlinear and has a specific point at which the power has its maximum value. This point is called the maximum power point (MPP). Therefore, an effective method for tracking the MPP is necessary to force the photovoltaic system to operate at this point in all weather conditions [4]. MPPT is one of the main components of photovoltaic systems. In recent years, various techniques and methods have been proposed by researchers to track the MPP. Methods based on the relationship between MPP voltage and open-circuit voltage, or MPP current and short-circuit current are presented in literature [5, 6]. The drawback of this method is that some energy will be lost during the short-circuit and the open-circuit. Another common method is perturbation and observation (P&O). In P&O, first the current and voltage and consequently the power (P_1) are measured. By creating a perturbation in voltage or current in a certain direction, the power will be measured again (P_2). Then, P_2 is compared with P_1; if P_2 is more than P_1, then the deviation is in the right direction; otherwise, it must be reversed. In this way, the maximum power point (P_{mpp}) and consequently the optimal point voltage (V_{mpp}) will be obtaine [7-9]. P&O-based techniques have been widely acclaimed due to their simplicity and ease of implementation, although these techniques are limited to the inherent nature of oscillation

*Corresponding Author Institutional Email: yaghobi@semnan.ac.ir
(H. Yaghobi)

Please cite this article as: M. Hooshmand, H. Yaghobi, M. Jazaeri, Irradiation and Temperature Estimation with a New Extended Kalman Particle Filter for Maximum Power Point Tracking in Photovoltaic Systems, ***International Journal of Engineering, Transactions C: Aspects***, Vol. 36, No. 06, (2023), 1099-1113

and noise in the system. Another common method is hill climbing (HC). The basic operation of this method is the same as P&O, but instead of perturbing the current or voltage, the duty cycle is perturbed to update the PV operating point. This algorithm can work based on fixed or variable step [10]. Due to the similarity, this method has the same advantages and drawbacks as P&O method does. Another common method that is widely used is InC. In this method, the slope of the P-V characteristic of the PV module is used to track the MPP. This method is based on the fact that the slope of the P-V characteristic is zero at the maximum power point, positive for output power less than MPP, and negative for output power greater than MPP. The MPP is obtained by deriving the output power function, with respect to the voltage, and setting it equal to zero. In fact, this method is performed by a stepwise comparison of the ratio of conductance derivative (dI/dV) with instantaneous conductance (I / V) [11, 12]. The InC method overcomes the inherent oscillation of the P&O method, although it is difficult to be implemented due to the presence of noise in the system. The aforementioned common methods are not accurate in rapid tracking of irradiation changes. Also, the presence of noise in real systems affects the performance of these methods. These methods are mainly used in combination with other methods [13, 14]. Also, different techniques are used to eliminate noise, which will result in the complexity of the system as well as the slowness of the tracker.

The attractiveness of the methods based on classical control theories and control concepts has prompted researchers to use some of these methods to track the maximum power point in PV systems. These methods are based on the mathematical model of the PV system and need the information of its parameters. The most common of these methods is the Kalman filter, which is widely used to estimate PV systems states. MPP tracking using the Kalman filter has been developed by Boutabba et al. [15], Motahhir et al. [16] and Farrokhi et al. [17]. Because of using Kalman filter, these methods are robust against noise. But due to linearization, the estimation error is significant. Owing to the severe nonlinearity of PV system equations, nonlinear versions of the Kalman filter (extended Kalman filter (EKF), Unscented Kalman Filter (UKF), etc.) have been developed for MPP tracking. Methods based on UKF stated by Abdelsalam et al. [18], EKF by Docimo et al. [19], and multiple model Kalman filter (MMKF) by Kumar et al. [20] have been proposed to estimate the states of PV systems for MPP tracking. In linear systems, the Kalman filter is the optimal estimator. Nonlinear versions of the Kalman filter can be used for nonlinear systems with Gaussian noise, but there is no reason for convergence and no proof that the resulting estimate is optimal. A method based on Bayesian inference is presented by Lefevre et al. [21] for MPP tracking, in this method there is no limitation on the type of system (linear or nonlinear). Also, this method does not make any assumptions for the probability density function (PDF) of the process noise and measurement noises, and does not need to use temperature and irradiation sensors. This method has good performance, but since integration is done on probability distribution functions; it is very difficult to calculate them, so it requires a powerful computer processor. Using a hardware that can perform these calculations will greatly increase costs. Simon [22] has proposed particle filter to overcome the limitations of Kalman filter. This estimator has optimal estimation in linear and nonlinear models. It has more improved performance compared to nonlinear versions of the Kalman filter. It makes no assumptions for the PDF of the noise, and can perform well for both non-Gaussian and Gaussian noises. Considering the mentioned characteristics and the presence of non-Gaussian noise in the industry, it seems that the estimation of the states of PV systems (which have severe nonlinearity) based on particle filter is suitable for MPP tracking.

In this paper, a new MPP tracking method, which is based on irradiation and module temperature estimation, is proposed. The estimation is done with a new EKPF. Since the basis of the proposed estimation method is the particle filter, the target system can be nonlinear and there is no assumption for the PDF of the noise. Due to the use of the combination of Kalman and particle filters, the estimation accuracy has been greatly improved compared to the common methods based on the Kalman filter. This method tracks MPP quickly and has good performance in dynamic and static modes. In this method, expensive radiation and temperature sensors are not used. The structure of this paper is as follows: in section 2, the thermal and electrical models of the PV module are presented. The state space equations are explained in section 3. In section 4, the proposed MPPT method is presented. First, EKF and particle filter are introduced, then the proposed estimation method is described, and subsequently, the new V_{mppt} calculation method that uses the estimated values of temperature and irradiation is presented. In section 5, the simulation setup is explained. The simulations are done in MATLAB/SIMULINK. In section 6, the results are discussed, which confirm the effectiveness of the proposed method. Finally, in section 7, conclusions are presented.

2. THE CHARACTERISTICS OF PHOTOVOLTAIC MODULES

Photovoltaic cells use semiconductor materials to convert sunlight into electricity. The technology is very close to solid-state technology, which is used to make transistors and diodes. When a piece of p-type silicon, that is lightly

doped with boron, and n-type silicon, that is heavily doped with phosphorus, are brought together, a p-n junction is formed. When a photon is absorbed, an electron-hole pair is produced in the p-type region. Due to the built-in electric field, which points towards the p-type region, the electrons drift into the n-type region and the hole remains in place. By electrically connecting the two terminals of the p-n junction, almost all the electrons produced by the photon migrate to the n-type region through the connecting wire; thus, completing the circuit. Since each photovoltaic cell produces only about 0.5 volts, it is rarely used alone. By connecting the cells in series, a compact form called a module, which has more applications and is resistant to harsh weather conditions, is formed [23]. The output voltage and current of the module depend on such factors as the amount of irradiation and the module temperature. So, to analyze and study these effects, two electrical and thermal models for the module are required. These will be described in the next sections.

2. 1. Electrical Model Among the PV module models, the two models of single-diode and two-diode have been used in literature [24, 25]. Comparisons between single-diode and two-diode models show that both models have acceptable accuracy. Although the two-diode model is slightly more accurate, it has been used less frequently in research due to its high complexity. In contrast, due to the fact that the single-diode model requires fewer calculations and has a smaller number of parameters, it has been widely used in research articles [26, 27]. This paper uses a single-diode model that, while simple, is accurate enough. Figure 1 shows a single-diode equivalent circuit of a PV module. In general, the resistance of R_s series is very small and the parallel resistance of R_p is very large and it is often neglected [28]. Due to the presence of diodes in this equivalent circuit, current and voltage equations are nonlinear. The output current of the module is calculated according to Equations (1) to (4).

$$I = I_{pv} - I_d - I_p \tag{1}$$

$$I_{pv} = (I_{pv,n} + K_I (T - T_n)) G / G_n \tag{2}$$

$$I_d = I_0 (\exp(q \frac{V + R_s I}{N_s kTa}) - 1) \tag{3}$$

$$I_0 = \frac{I_{sc,n} + K_I (T - T_n)}{\exp(q \frac{V_{oc,n} + K_v (T - T_n)}{N_s kTa}) - 1} \tag{4}$$

where, I_{pv}, I_d, I_p, and I_0 are the photovoltaic current, diode current, parallel branch current, and diode saturation current, respectively. V and I are the voltage across the terminal and the module current, respectively.

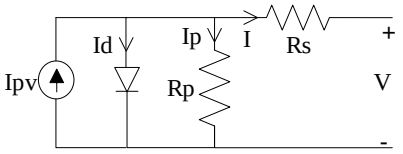

Figure 1. The equivalent circuit of the PV module

T and G are the module temperature (in Kelvin) and the amount of irradiation (in kw/m^2), respectively. T_n and G_n are the nominal values of ambient temperature and irradiation, respectively. $V_{oc,n}$, $I_{sc,n}$, and $I_{pv,n}$ are the open-circuit voltage, short-circuit current, and photovoltaic current in standard irradiation and temperature, respectively. q is the charge of an electron, k is the Boltzmann constant, and parameter a is the diode ideality constant. The K_i and K_v constants indicate the relationship between the module temperature with the short-circuit current and the module temperature with the open-circuit voltage, respectively. Based on Equations (1) to (4), the I-V and P-V characteristic curves of the module are shown in Figure 2. In this figure, the effect of temperature and irradiation changes on the I-V and P-V curves as well as the MPP are specified.

2. 2. Thermal Model As shown in Figure 2 (c and d), the module temperature is one of the determining quantities of the MPP point in photovoltaic systems, so a suitable thermal model of photovoltaic modules is needed to determine MMP point. Different models are presented by Jones and Underwood [29], Mattei et al. [30] and Abdelhameed et al. [31] based on energy balance, multilayer model, and a model for hot spot conditions. In this work a thermal model, which is based on the simple method of energy balance, has been used. The photovoltaic module is approximated as a lumped capacity with a uniform temperature and the irradiation exchange between the module and its environment is neglected. After the sun radiates on the surface of the module, some of it is converted into electrical power by photovoltaic cells, and some of it changes the temperature of the module. Considering the amount of irradiation, the absorption coefficient, and heat exchange between the module and the surrounding environment, whether in the form of natural or forced convection, the final temperature of the module is determined. With these assumptions, the heat transfer equations of the PV module stated as follows:

$$\dot{x}_1 = (q_{sw} - q_{conv} - P_{out}) / C_m \tag{5}$$

$$\begin{cases} q_{sw} = \alpha A_s w_1 \\ q_{conv} = A_s (h_{free} + h_{forced})(x_1 - w_2) \\ P_{out} = V_m I_m \end{cases} \tag{6}$$

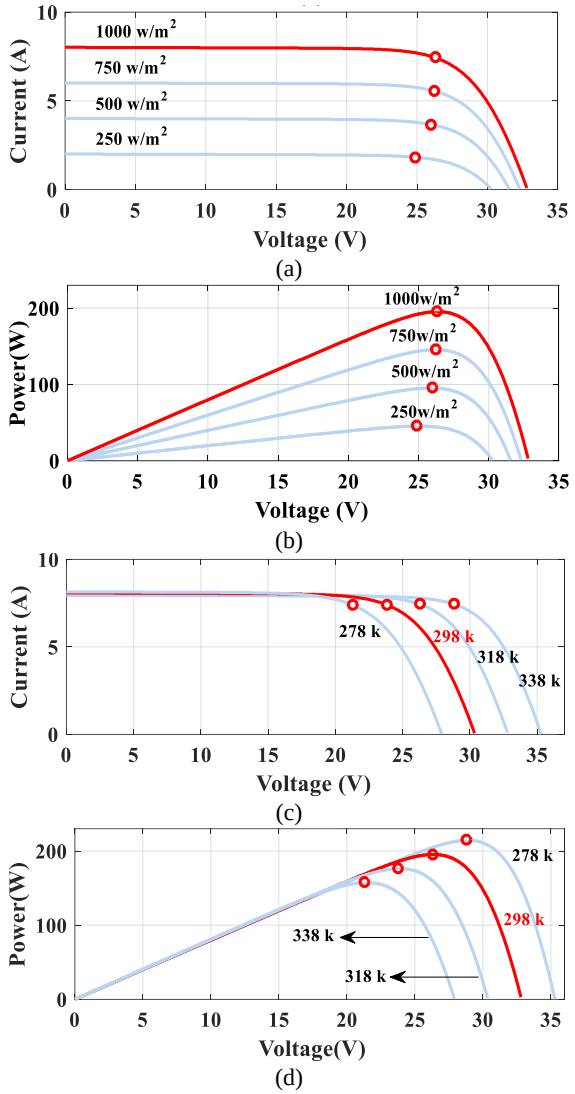

Figure 2. (a) and (b) I-V and P-V characteristic curves, respectively, for various irradiation and T = 298 k, (b) and (d) I-V and P-V characteristic curves for various temperature and Irr = 1000 w/m^2

$$\begin{cases} h_{free} = 1.31(x_1 - w_2)^{1/3} \\ h_{forced} = 5.67 + 3.86 w_3 \end{cases} \quad (7)$$

where, x_1 and w_2 are the module temperature and the ambient temperature, respectively. w_1 and w_3 are the irradiation value and wind speed in the area, V_m is the module voltage that is determined using MPP tracker, I_m is the output current of the module, which is multiplied by the voltage at which the output power (P_{out}) is obtained. Other parameters are described in Table 1. By combining Equations (5) to (7), the final equation of temperature changes will be calculated according to the climatic conditions of the region and the output power of the module as:

TABLE 1. Parameters of the Thermal Model of the PV Module

Parameter	Description
C_m	lumped thermal capacitance
q_{sw}	Short-wave radiation
q_{conv}	free and forced convection
A_s	module's surface area
A	Absorptivity
h_{free}	free convection coefficients
h_{forced}	forced convection coefficients

$$\dot{x}_1 = \frac{1}{C_m}(\alpha A_s w_1 - A_s(1.31(x_1 - w_2)^{1/3} + 5.67 + 3.86 w_3) \times (x_1 - w_2) - V_m I_m) \quad (8)$$

3. STATE SPACE EQUATIONS

The irradiance during a clear day follows a sinusoidal pattern. In this work, x_2 and x_3 states are used to model irradiation. Irradiation state equations are presented in Equation (9).

$$\begin{cases} \dot{x}_2 = x_3 + \Omega \\ \dot{x}_3 = -f^2 x_2 \\ x_2(0) = 0, x_3(0) = Af \end{cases} \quad (9)$$

where x_2 is irradiation value, f represents the frequency of the sine wave and depends on the number of sunny hours during the day, and A is the peak of irradiation during the day. Cloud cover changes affect the amount of solar irradiation on the photovoltaic module and it causes the irradiation to deviate from the sinusoidal shape. To consider these conditions, process noise Ω will be used in the equations, that is added to the irradiation state equation, as presented in this equation. By substituting Equation (2) to Equation (4) into Equation (1) and transferring all the factors to the left of the equation, the output current equation will be obtained. Voltage and current values are measured with sensors with measurement noises v_{u2} and v_y. In Equation (1), by substituting $G = w_1$, $T = x_1$, $I = y$ and $V = u$; in Equation (8), by substituting $w_1 = x_2$, $I_m = y$ and $V_m = u$, the variables are unified. In Equation (8), the voltage has the process noise v_{u1} because the voltage cannot be completely controlled, the wind speed and ambient temperatures are measured with the noise sensors v_{w2} and v_{w3}, respectively. In this way, the state space equations are expressed as follows:

$$\begin{cases} \dot{X} = f(X, U, \omega) \\ g(X, u, y, \upsilon) = 0 \end{cases} \quad (10)$$

where in these equations, the input vector, noise vectors, state vector, and the probability distribution function of process noise and measurement noise are presented in Equation (11).

$$\begin{cases} U = [u, w_2, w_3], \omega = [\Omega, \upsilon_{u1}, \upsilon_{w2}, \upsilon_{w3}] \\ \Omega = N(0, \sigma_\Omega), \upsilon_{u1} = N(0, \sigma_{u1}) \\ \upsilon_{w2} = N(0, \sigma_{w2}), \upsilon_{w3} = N(0, \sigma_{w3}) \\ \upsilon = [\upsilon_{u2}, \upsilon_y], \upsilon_{u2} = N(0, \sigma_{u2}), \upsilon_y = N(0, \sigma_y) \\ X = [x_1, x_2, x_3] \end{cases} \quad (11)$$

4. PROPOSED MPPT METHOD

In this section, the proposed maximum power point tracking method is presented. The module temperature and irradiation are required to track the MPP. These values are estimated by the proposed method which is very accurate; they are plugged into Equations (1) to (4), and then the V_{mpp} value is calculated through a new technique and applied to the converter. Highly accurate estimates lead to accurate V_{mpp} calculations which improve efficiency, thereby increasing the daily energy generation of the photovoltaic system. In this section, the conventional EKF, the standard particle filter, the proposed estimation method, and the proposed V_{mppt} calculation technique are presented, respectively.

4. 1. Extended Kalman Filter The Kalman filter uses recursive least squares (RLS) to estimate the states of linear systems in noisy environments. This filter uses time and measurement updates and it works recursively and over time. The effect of noise on the system is reduced due to the recursive cycle and finally leads to the actual measurement value [22]. The EKF is a non-linear version of the Kalman filter and is suitable for nonlinear systems. The system is linearized around the point of the previous step, and after extracting the equations, the linear Kalman filter is applied to it. System equations are assumed as Equation (12).

$$\begin{cases} x_k = f_{k-1}(x_{k-1}, u_{k-1}, \omega_{k-1}) \\ y_k = h_k(x_k, u_k, \upsilon_k) \\ \omega_k \approx N(0, Q_k) \\ \upsilon_k \approx N(0, R_k) \end{cases} \quad (12)$$

where $x_k \epsilon R_n$ is the state of the system, and $y_k \epsilon R_m$ is the measured output of the system in step k. ω and υ are process and measurement noise, respectively; which have Gaussian PDF, with zero mean value, and covariance matrices Q and R. u and y are the input and output of the system, respectively. *f(..)* and *h(..)* are the nonlinear functions of the system and measurement, respectively. Assuming that the equations of the system are in the form of Equation (12), the state's estimation of the system is obtained through the following steps.

a. Initializing

$$\begin{cases} \hat{x}_0^+ = E(x_0) \\ P_0^+ = E[(x_0 - \hat{x}_0^+)(x_0 - \hat{x}_0^+)^T] \end{cases} \quad (13)$$

b. Time update stage

$$\begin{cases} F_{k-1} = \left.\dfrac{\partial f_{k-1}}{\partial x}\right|_{\hat{x}_{k-1}^+} \\ L_{k-1} = \left.\dfrac{\partial f_{k-1}}{\partial \omega}\right|_{\hat{x}_{k-1}^+} \\ P_k^- = F_{k-1} P_{k-1}^+ F_{k-1}^T + L_{k-1} Q_{k-1} L_{k-1}^T \\ \hat{x}_k^- = f_{k-1}(\hat{x}_{k-1}^+, u_{k-1}, 0) \end{cases} \quad (14)$$

c. Measurement update stage

$$\begin{cases} H_k = \left.\dfrac{\partial h_k}{\partial x}\right|_{\hat{x}_k^-} \\ M_k = \left.\dfrac{\partial h_k}{\partial \upsilon}\right|_{\hat{x}_k^-} \\ K_k = P_k^- H_k^T (H_k P_k^- H_k^T + M_k R_k M_k^T)^{-1} \\ \hat{x}_k^+ = \hat{x}_k^- + K_k[y_k - h_k(\hat{x}_k^-, u_k, 0)] \\ P_k^+ = (I - K_k H_k) P_k^- \end{cases} \quad (15)$$

where $\hat{x}_k^-$ and $\hat{x}_{k-1}^+$ are the estimation of states in k and k-*1*, time step, respectively. The "+" and "-" superscripts indicate the posteriori and priori estimates, respectively. P_k is the error covariance matrix in the time step k, and K_k is Kalman gain.

4. 2. Standard Particle Filter Particle filtering is a statistical method for estimating states. This filter is often used to estimate the states of systems with severe nonlinearity. The particle filter is based on the Bayesian state estimator. In fact, the purpose of this estimator is to find the PDF of the states assuming measurements y_1, y_2, …, y_k, and the initial conditions x_0. The Bayesian state estimator has two steps: the calculation of the priori and posteriori PDF, respectively, and in accordance with Equations (16) and (17).

$$p(x_k \mid Y_{k-1}) = \int p(x_k \mid x_{k-1}) p(x_{k-1} \mid Y_{k-1}) dx_{k-1} \quad Y_{k-1} = y_1, y_2, \ldots y_{k-1} \quad (16)$$

$$p(x_k \mid Y_k) = \frac{p(y_k \mid x_k) p(x_k \mid Y_{k-1})}{\int p(y_k \mid x_k) p(x_k \mid Y_{k-1}) dx_k} \quad Y_k = y_1, y_2, \ldots y_k \quad (17)$$

In these equations, integration is performed on probability distribution functions. Normally, the

analytical response of these equations is very difficult due to the large dimensions of the state space and can only be calculated for very specific systems. The numerical calculation of these integrals is also a very tedious and time-consuming task. The particle filter solves this problem; in fact, the particle filter has been developed to numerically implement the Bayesian state estimator. This filter estimates signals by sampling, these samples are called particles [32-34]. The sampling process is performed on the system's dynamic equation, and the samples are weighted using the measurement equation, then based on these samples and their weights, the optimal estimate of the stochastic signal is obtained. System equations are assumed to be as Equation (10). The PDF of the process noise (ω) and the measurement noise (υ) are not necessarily Gaussian, and just knowing the distribution is enough and the type of distribution is not important. With these assumptions, the particle filter algorithm estimates the states of the system as follows [33, 34]. In these steps, note that *p(..)* means the probability distribution function, not the probability value. The index *i* is the particle number, index *k* is the time step ($k = 0,1\ldots$), and the superscripts "-" and "+" represent the priori and posteriori estimates, respectively.

1. Assuming that the initial PDF of the state $p(x_0)$ is known, first the N vector is generated randomly, and based on the initial PDF $p(x_0)$, these vectors are called particles and are denoted by $x_{0,i}^{+}(i=1,...,N)$. The N parameter is a trade-off between the estimate accuracy and the amount of calculations and is determined by the designer.
2. In each time step $k = 1, 2, \ldots$ the following steps will be performed.

a. Using the nonlinear equation of the system (f(..)) and the known PDF of the process noise, the time propagation is performed to calculate the priori particles by Equation (18).

$$x_{k,i}^{-} = f_{k-1}(x_{k-1}^{+}, u_{k-1} w_{k-1}^{j}) \qquad (i=1,...,N) \tag{18}$$

In this equation, each noise vector is generated randomly based on a known PDF of w_{k-1}.

b. Once the measurement in step k is received, the relative likelihood q_i of each particle conditioned on the measurement y_k is calculated. This is done by evaluating the PDF (p(yk|x-k,i)) based on the nonlinear measurement equation (h(..)) and the specified PDF of the measurment noise.

c. The resulting likelihoods are normalized based on the following equation.

$$\bar{q}_i = \frac{q_i}{\sum_{j=1}^{N} q_j} \tag{19}$$

The sum of the total likelihood is now equal to one.

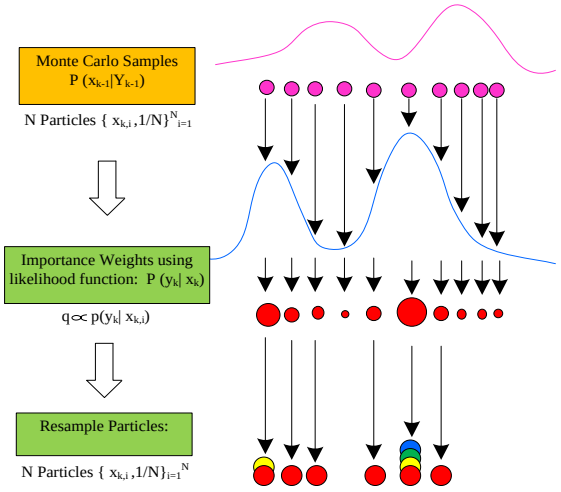

Figure 3. SIR method in solving particle impoverishment problem [33]

d. Posteriori particles $x_{k,i}^{+}$ are produced based on q_i likelihoods. This step is called re-sampling. This is possible in several ways. The particle impoverishment is one of the problems that the process of sampling and signal estimation will face with if improper methods are used; however, the resampling algorithm is used to solve it. Figure 3 shows the most common SIR algorithm. In this method when $N_{eff} = 1/\sum_{i=1}^{N} \bar{q}_i^{\,2} < N_{thr}$ the resampling operation is performed in such a way that the weight of all the samples is converted to *1/N* and then the re-weighing is performed. In this way, less valuable samples are automatically removed after a few steps.

e. We now have a set of new particles $x_{k,i}^{+}$ distributed according to $p(x_k|y_k)$, so we can calculate any statistical criterion of this PDF. We are often only interested in calculating the mean and the covariance.

4. 3. Proposed Estimation Method To improve the performance of the particle filter, one of the proposed methods is to combine it with non-linear versions of the Kalman filter (EKF, UKF or CKF). In the proposed estimation method, the improved particle filter is combined with EKF. In the proposed method, particle classification is used in the resampling step. This makes the proposed combined filter very accurate in estimating system states, even if the system has severe nonlinearity. The proposed method in this paper is named EKPF in short. In this approach, each particle is updated by the EKF at the measurement time, and then resampling is performed using the measurement. In the proposed method, there is no assumption for the probability density functions. This method works correctly for Gaussian and

non-Gaussian noises. The steps of this method are as follows;

1. Equations of system and measurement are assumed according to Equation (10). Independent white noises ω_k and v_k are considered with specific PDF. The covariance matrices of the noises are defined as Equation (20).

$$Q = diag(\sigma_{\Omega}, \sigma_{u1}, \sigma_{w2}, \sigma_{w3})$$
$$R = diag(\sigma_{u2}, \sigma_{y}) \quad (20)$$

2. It is assumed that the initial PDF of system states is p(x0). Based on this PDF, N number of primary particles are produced randomly. For i = 1, ..., N, these particles are named $x_{0,i}^{+}$ and their covariance is named $P_{0,i}^{+} = P_0^{+}$. The number of particles is determined based on the trade-off between the calculations amount and the accuracy of the estimation.
3. The following steps are performed for $k = 1, 2, \ldots$.

a. The time propagation step is performed using the known PDF of the process noise and the known process equation, to obtain a priori particles $x_{0,i}^{+}$ and covariances $P_{k,i}^{-}$.

$$\begin{cases} F_{k-1,i} = \left.\dfrac{\partial f_{k-1}}{\partial X}\right|_{x=x_{k-1,i}^{+}} \\ L_{k-1,i} = \left.\dfrac{\partial f_{k-1}}{\partial \omega}\right|_{x=x_{k-1,i}^{+}} \\ \hat{x}_{k,i}^{-} = f_{k-1}(\hat{x}_{k-1,i}^{+}, u_{k-1}, w_{2k-1,i}, w_{3k-1,i}, \omega_{k-1}^{+}) \\ P_{k,i}^{-} = F_{k-1,i} P_{k-1,i}^{+} F_{k-1,i}^{T} + L_{k-1,i} Q_{k-1} L_{k-1,i}^{T} \end{cases} \quad (21)$$

where ω_{k-1}^{i} noise vector is generated randomly based on the known PDF of ω_{k-1}, and L and F are Jacobin matrices.

b. The priori particles and their covariance are updated and their posteriori values are obtained by Equation (22)

$$\begin{cases} H_{k,i} = -\dfrac{\partial g_k}{\partial X}\left(\dfrac{\partial g_k}{\partial y}\right)^{-1}\Big|_{x=x_{k,i}^{-}} \\ M_{k,i} = -\dfrac{\partial g_k}{\partial \upsilon}\left(\dfrac{\partial g_k}{\partial y}\right)^{-1}\Big|_{x=x_{k,i}^{-}} \\ K_{k,i} = P_{k,i}^{-} H_{k,i}^{T} (H_{k,i} P_{k,i}^{-} H_{k,i}^{T} + M_{k,i} R_k M_{k,i}^{T})^{-1} \\ \hat{x}_{k,i}^{+} = \hat{x}_{k,i}^{-} + K_{k,i}[y_{k,i} - \hat{y}_{k,i}] \\ P_{k,i}^{+} = (I - K_{k,i} H_{k,i}) P_{k,i}^{-} \end{cases} \quad (22)$$

where H and M are Jacobian matrices, and K is the Kalman gain for $i^{'}th$ particle. y_k is found at the reference point by solving the output Equation (10).

c. The relative likelihood q_i of each posteriori particle $x_{k,i}^{+}$ is calculated under the condition of measurement y_k. This is done by evaluating the PDF $p(y_k \mid x_{k,i}^{+})$, based on the nonlinear measurement equation g and the PDF of the measurement noises.

d. The relative likelihoods obtained from the previous step are scaled by Equation (19). Now the sum of all of them equals to one.

e. Based on the calculated likelihoods and the following resampling method, the posterior particles $x_{k,i}^{+}$ and the covariance $P_{k,i}^{+}$ will be refined.

The adopted resampling algorithm is that the particles are divided into three classes based on their weight. The values of the maximum and minimum thresholds (q_{trmax} and q_{trmin}), i. e. the boundary between the classes, are defined. The samples will be classified according to Equation (23).

$$\tilde{x}_{k+1} = \begin{cases} 0 & \tilde{q}_{k,i} < q_{thr\,\min} \\ x_{k+1} & q_{thr\,\min} < \tilde{q}_{k,i} < q_{thr\,\max} \\ fission & \tilde{q}_{k,i} > q_{thr\,\min} \end{cases} \quad (23)$$

And then, if $N_{eff} \leq N_{thr}$, the resampling step is done. It is assumed that the P particles are in the first class. K is the number of particles in the second class and the N-P-K particles are in the third class. Class 1 particles are removed, class 2 particles remain unchanged, and class 3 particles are divided into several particles according to their weight and Equation (24)

$$m_i = [q_{k,i}(N - P - k)] \qquad i = 1, 2, \ldots N - P - K \quad (24)$$

where m is the number of particles produced based on weight $q_{k,i}$ and [..] is the integer function. In this algorithm, the breaking method is used, and to calculate the weight of the broken particles, relation (25) will be used.

$$q_{k,i'} = q_{k-1,i} \times p(y_k \mid x_{k,i'}) \quad (25)$$

Figure 4 shows the particle classification process.

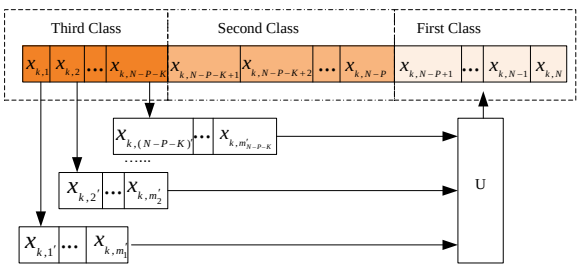

Figure 4. Particle weight classification process

f. We now have a set of new particles $x_{k,i}^{+}$ distributed according to $p(x_k|y_k)$, so we can calculate any statistical criterion of this PDF. Figure 5 shows the general algorithm of the proposed estimation method.

4. 4. Proposed V_{mppt} Calculation Method As shown in Figure 2, the PV module has different P-V characteristics for different amounts of irradiation and temperature, each with a different V_{mppt} value. Therefore, the irradiation and module temperature are two important quantities in determining the MPP. After each measurement, the proposed estimation method estimates the irradiation and module temperature. The tracker uses these values as input and determines the V_{mppt} based on the P-V equations. This is done by deriving the power equation, with respect to the voltage, and setting it to zero. By multiplying the two sides of Equation (1) by V, we have:

$$V \times I = V \times (I_{pv} - I_0(\exp(q\frac{V + R_s I}{N_s kTa}) - 1) - \frac{V + R_s I}{R_p})) \quad (26)$$

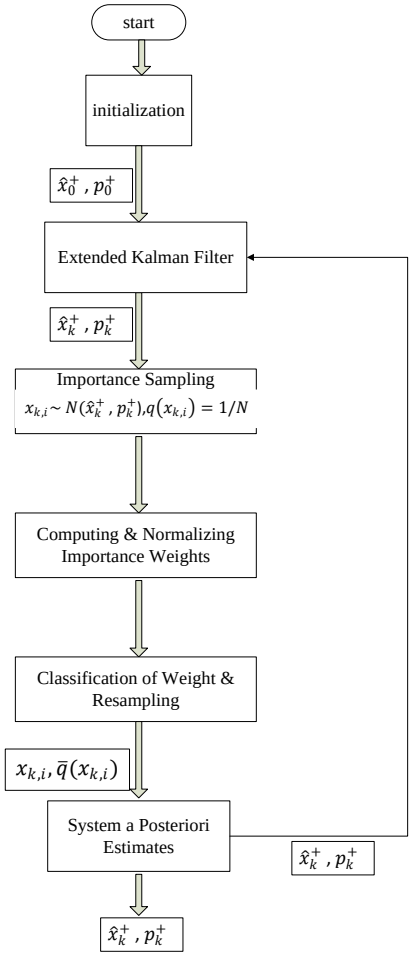

Figure 5. The proposed estimation algorithm

By replacing $I = P/V$ we have:

$$P - V(I_{pv} - I_0(\exp(q\frac{V + R_s P/V}{N_s kTa}) - 1) - \frac{V + R_s P/V}{R_p}) = 0 \Rightarrow g(P,V) = 0 \quad (27)$$

By deriving P, with respect to V, we have:

$$\frac{dP}{dV} = -\frac{\partial g}{\partial V}(\frac{\partial g}{\partial P})^{-1} = 0 \quad (28)$$

where V and P are inseparable. This equation is solved by numerical methods in a certain voltage range. In this work, the Newton-Raphson method is used to solve the equation, because this method converges rapidly. The resulting voltage is immediately applied to the DC/ DC converter to achieve maximum power. The voltage is kept constant until the next measurement is obtained. In this method, no data is stored, so no memory is required to store the data. Storing more data is a burden over any numerical solution. Therefore, this method is superior to the methods based on look-up table.

5. SIMULATION SETUP

The configuration of the simulation setup is shown in Figure 6. Climatic conditions (wind, sunlight, etc.) are applied to the module by the environment. The values of wind speed, ambient temperature, voltage and current are measured by sensors, then each of these quantities, which has an independent noise, are applied to the estimator. Estimation by the proposed method determines the amount of irradiation and module temperature. These values are applied as input to the MPP Tracker to determine the optimal point. No assumptions are made for noise distribution in the proposed method, but to be able to compare the proposed method with the EKF method, we assume that the noise is Gaussian. All variance values of noise, as well as initial values of

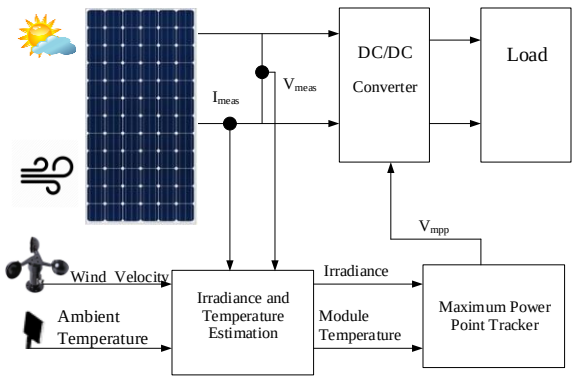

Figure 6. Simulation setup configuration

covariance and system states, are similar to the values reported in the literature [19].

It is assumed that all noises are uncorrelated and have zero mean value, although there is no need for this, and correlated noises with a non-zero mean value can be used with small changes in the equations. All values of noise variance are presented in Table 2. The initial values of the states and error covariances are presented in Equations (29) and (30), which are the expected values at the beginning of the PV module operation.

$$\hat{x}_{0|0} = \left[\tilde{w}_0(0), 0, (1000 W/m^2) f \right]^T \quad (29)$$

$$P_{0|0} = diag\left((3k)^2, (50 W/m^2)^2, (0.02 \frac{W}{m^2} \frac{rad}{s})^2 \right) \quad (30)$$

A 250-watt module is used for simulation. All values of the parameters of the electric and thermal models are shown in Table 3. Environmental inputs for simulation, including irradiation, wind speed, and ambient temperature, have been obtained from the National Wind Technology Center (NWTC, 2016). Three sets of M2 tower data in Boulder, Colorado have been used. Dates are selected in a way that different weather conditions could be applied to the system. A day with a clear sky (May 28, 2014), a partly cloudy day (May 13, 2014), and a severely cloudy day (May 11, 2014) have been chosen. The values of irradiation, ambient temperature, and wind speed on the dates mentioned are shown in Figure 7. These values are used in Equations (2) and (8) to calculate the actual values of radiation and module temperature.

TABLE 2. Noise variance values

Variance	Value
$\sum_{w2}$	$(0.1\ K)^2$
$\sum_{w3}$	$(1 m/s)^2$
$\sum_{u1}$	$(0.1V)^2$
$\sum_{u2}$	$(0.01V)^2$
$\sum_{y}$	$(0.05A)^2$
$\sum_{\Omega}$	$(1 W/m^2 s)^2$

TABLE 3. System Parameters

Parameter	Value
A_s	0.8 (m^2)
C_m	4580 (J/K)
$I_{pv,n}$	8.02 (A)
K_i	0.0032 (A/K)
T_n	298 (k)
G_n	1000 ($W/m2$)
$I_{sc,n}$	8.21 (A)
q	$1.60217646*10^{-19}$ (C)
$V_{oc,n}$	32.9 (V)
K_v	-0.1230 (V/K)
a	1.3
N_s	54
k	$1.3806503*10^{-23}$ (J/K)
R_s	0.221 (Ω)
R_p	415.405 (Ω)
α	0.7

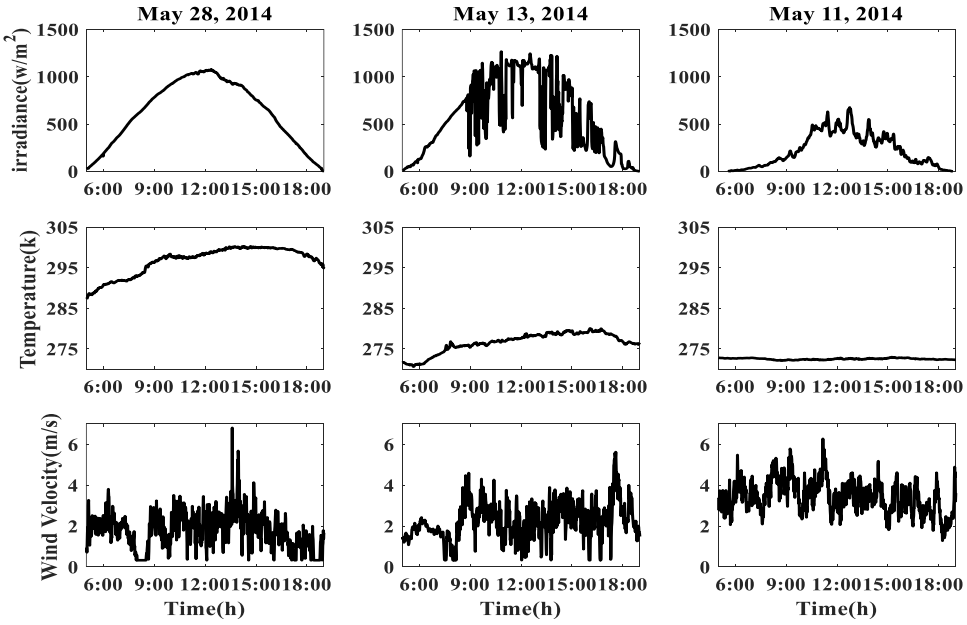

Figure7. Values of wind speed, irradiation, and ambient temperature on May 28, May 13, and May 11 2014

Given that the data is measured for every minute, the simulation step will be 60 seconds. The system's continuous equations are discretized by the Euler method with a time step of T=60 s. The number of particles in the simulation is considered to be N=100.

6. SIMULATION RESULTS

In order to confirm the accuracy of the estimated values, the proposed estimation method was compared with the common estimation method based on EKF. Both methods are simulated in similar atmospheric conditions. Gaussian noise with variance values presented in Table 2 was applied to both methods. The root means square error (RMSE) criterion will be used to compare the estimation error. Since the irradiation and module temperature are accurately estimated, the MPP is tracked with good accuracy in the proposed method. To verify this, the proposed method is compared with the EKF-based method and the common traditional method of InC in terms of the generated power. Also, these methods were compared in terms of efficiency, which can be calculated from Equation (31)

$$\eta_{mpp} = \frac{\sum_j i_{meas,j} v_{meas,j} \Delta t_j}{\sum_k i_{MPP,k} v_{MPP,k} \Delta t_k} \quad (31)$$

where i_{meas} and v_{meas} are the current and voltage of the PV module during the j'th time interval (Δtj), respectively. i_{MPP} and v_{MPP} are the current and voltage of the MPP during the k'th time interval (Δt_k), respectively. The methods were compared in different weather conditions, a day with a clear sky, a partly cloudy day, and a severely cloudy day.

6. 1. Clear Skies The data for this condition is shown in Figure 7 for 28 May 2014. From top to bottom, the amount of radiation, ambient temperature and wind speed during the day are shown in this figure, respectively. As seen in the figure, the irradiation follows a sinusoidal trend. Figure 8 shows the performance of irradiation and temperature estimation with the proposed estimation method and EKF. As can be seen in Figures 8 (a and b), the temperature estimation error in the proposed method (except for the case of initial conditions) is less than 0.2K, while it is about 5K in EKF. The RMSE in the proposed method is 0.0053, which, compared to the number 0.04 for the EKF method, indicates the appropriate accuracy of the proposed method in estimating the temperature. In Figures 8 (c and d), the real value of irradiation is compared with its estimated value by the proposed and EKF methods. Estimation errors in Figure 8(d) indicate that the maximum estimation error in the proposed method was 5W/m^2, while in the EKF method it is about 30 w/m^2. The RMSE value in the proposed method is 0.089, which indicates the accuracy of the proposed estimator, compared to the 0.258.

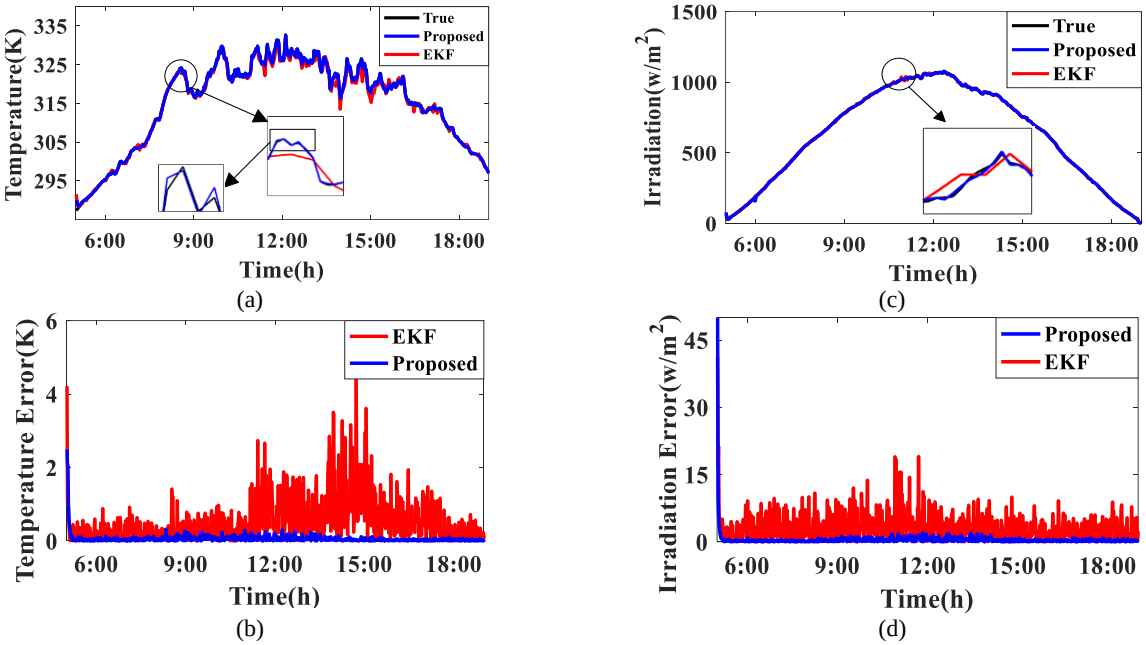

Figure 8. The comparison of actual and estimated values (Temperature and Irradiation) using the EKF and the proposed method in the first case (clear skies conditions- for May 28, 2014)

Figure 9 shows the generated maximum power of the PV module using the proposed method, the EKF-based method, and the InC method on a day with a clear sky in 2014. The results were compared with the real maximum power produced by the actual irradiation and module temperature. The error obtained from the three methods with the true power is also presented in this figure. The results show that in the proposed method, the maximum error is 0.1 watts, and for the EKF method, this value is increased to 1 watt and in the InC method it is about 6 watts. The proposed method has an efficiency of 99.99%, which is about 0.1% higher than the EKF method, and about 1% higher than the InC method. As a result, the proposed method produces 5.5 kJ more than the EKF method and about 50 kJ more than the InC method per day.

6. 2. The Partly Cloudy Sky Figure 7 shows the data for these conditions as of May 13, 2014. From top to bottom, the amount of radiation, ambient temperature and wind speed during the day are shown in this figure, respectively. Figure 10 shows a comparison of irradiation and temperature estimation performance using the proposed and EKF methods. The error in estimating the temperature in the proposed method (except for the case of initial conditions) in the semi-cloudy conditions is below 0.5 K, while it is about 4.5K in the EKF. The value of RMSE in the proposed method is 0.0027, which indicates the appropriate accuracy of the proposed estimator, compared to the number 0.029 for the EKF method. Figure 10 (c and d) shows the comparison of the real and estimated values of irradiation by the proposed and the EKF methods. Errors indicate that the maximum estimate error in the proposed method is 2.5 w/m^2, while it is about 28 w/m^2 in the EKF method. The value of RMSE in the proposed method is 0.065 and this value in EKF is 0.3.

Figure 11 shows the output power of the PV module using the proposed the EKF-based and the InC methods. The results were compared with the real maximum power generated by the actual irradiation and module temperature. The errors and their deviation from the true power are also presented in this figure. The results show that in the proposed method, the maximum output power error is less than 0.05 watts, and for the EKF method, this value is increased to 0.3 and in the InC method it is about 80 watts. The average efficiency of the proposed method is about 99.97, which is about 1.5% more than the EKF and about 7% more than the conventional InC method. This means that the proposed method generates about 33 kJ more than the EKF method and about 198 kJ more than the InC method daily.

6. 3. Severely Cloudy Skies The data for this condition is shown in Figure 7 for May 11, 2014. From top to bottom, the amount of radiation, ambient temperature and wind speed during the day are shown in this figure, respectively. Figure 12 shows a comparison of irradiation and temperature estimation performance with both the proposed and EKF methods. The maximum temperature estimation error in the proposed method (except for the case of initial conditions) is about 0.4 K,

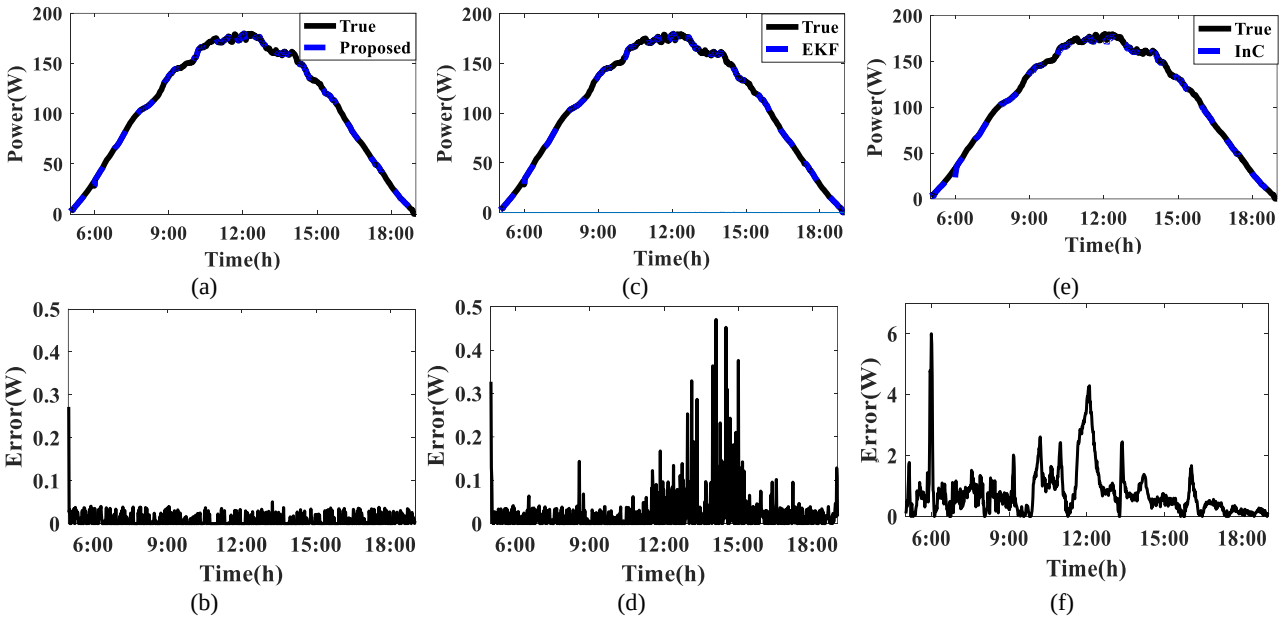

Figure 9. The comparison of the power generated by the PV module using the proposed method (a and b), EKF-based method (c and d), and InC method (e and f) in clear sky conditions

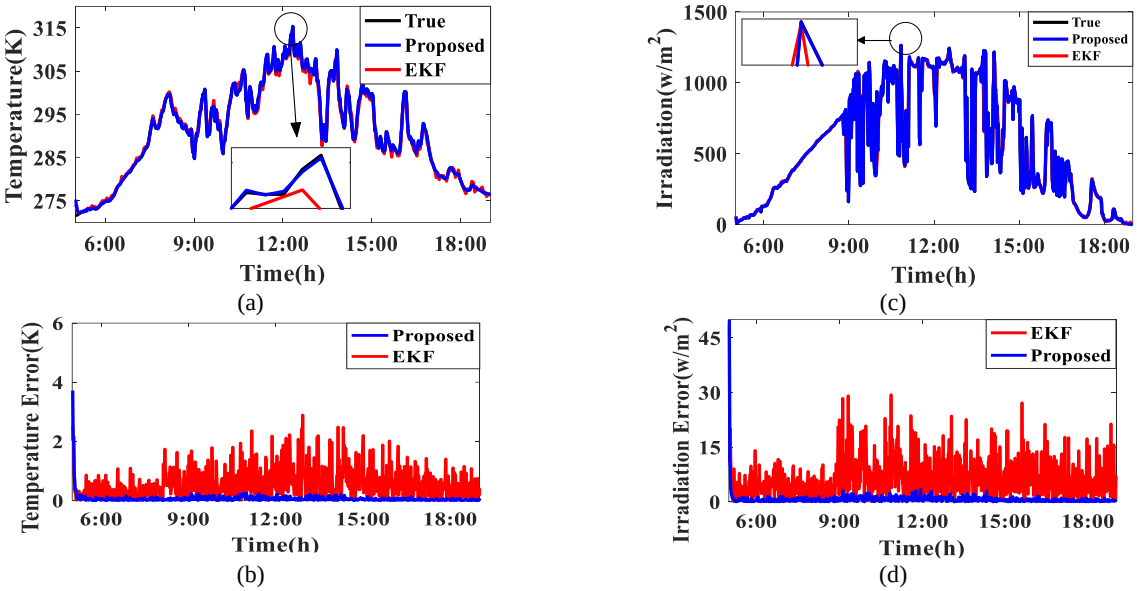

Figure 10. The comparison of actual and estimated values (Temperature and Irradiation) using the EKF and the proposed method in the second case (the partly cloudy sky conditions- for May 13, 2014)

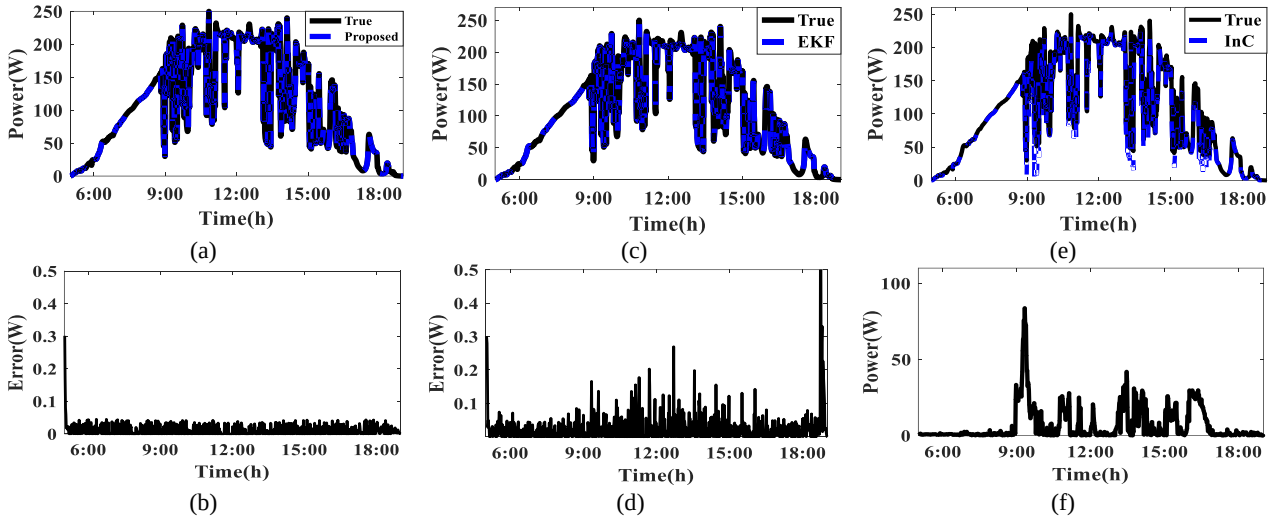

Figure 11. The comparison of the power generated by the PV module using the proposed method, InC method, and EKF-based method in partly cloudy conditions

while this value in the EKF method is about 3K. The RMSE in the proposed method is 0.006, which shows a very good accuracy of the proposed method in these weather conditions, compared to the 0.0179 for the EKF. Figure 12 (c and d) shows the comparison of the real and estimated values of irradiation by the proposed method and the EKF method. The maximum estimate error in the proposed method is 2w/m^2 and for EKF is about 40 w/m^2 approximately. The value of RMSE in both EKF and proposed estimation methods is 0.063 and 0.32, respectively, which indicates the appropriate accuracy of the proposed method. Figure 13 shows the output power of the PV module using the proposed method, the EKF-based method and the InC method. The results were compared with the real maximum power generated by the actual irradiation and module temperature. The results show that the error is 0.05 watts for the proposed method, 22 watts for InC, and approximately 0.3 watts for EKF. The proposed method has an efficiency of 99.96%, which is 0.15% more than the EKF method and 8.65% more than the InC method. This means that the proposed method produces about 5.1 kJ more than EKF and about 294 kJ more than InC per day. Table 4 presents the RMSE values for the proposed method and EKF, and the efficiency and daily energy production values for all methods (Proposed, EKF-based and InC).

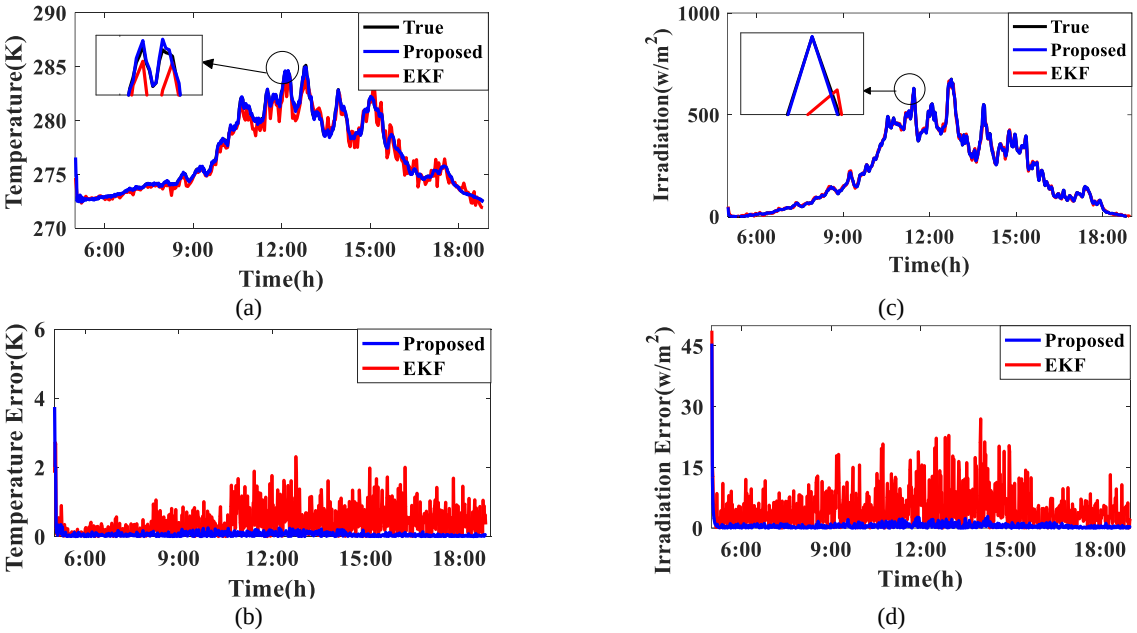

Figure 12. The comparison of actual and estimated values (Temperature and Irradiation) using the EKF method and the proposed method in the third case (the severely cloudy skies conditions- for May 11, 2014)

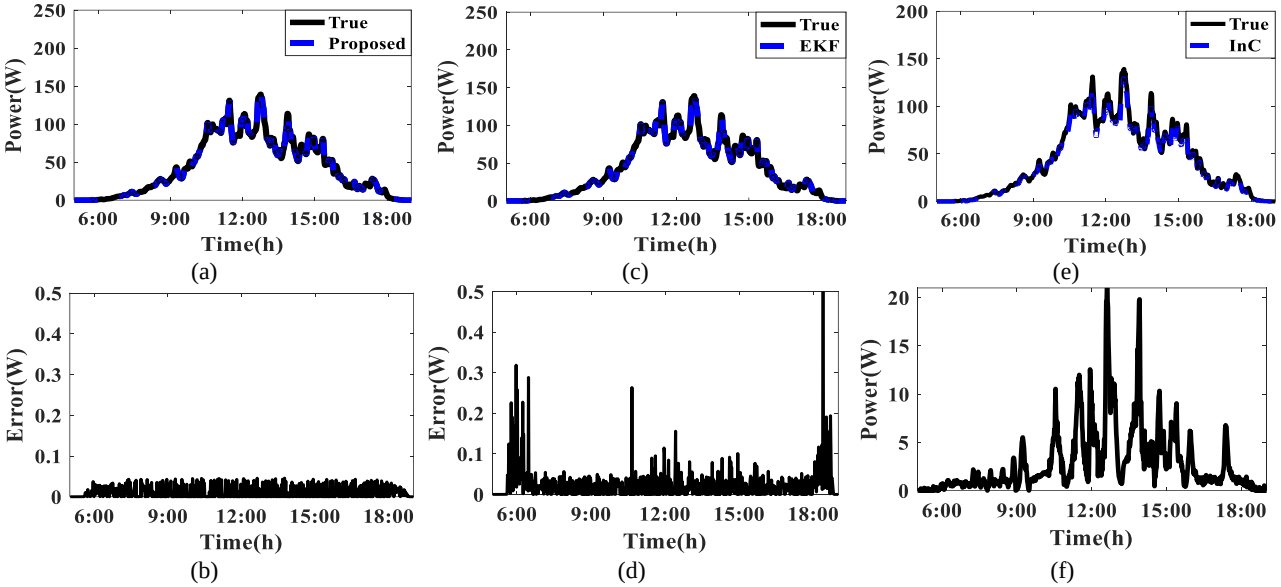

Figure 13. The comparison of the power generated by the PV module using the proposed method, InC method, and EKF-based method in severely cloudy conditions

TABLE 4. The Comparison of RMSE Value and Efficiency Value in the Proposed Method, EKF method and InC Method

Estimate Method	RMSE Value					
	Condition 1		Condition 2		Condition 3	
	T	*Irr*	*T*	*Irr*	*T*	*Irr*
EKF	0.04	0.258	0.029	0.3	0.0183	0.32
Proposed	0.0053	0.089	0.0027	0.065	0.0061	0.063

MPPT Method	Efficiency		
	Condition 1	Condition 2	Condition 3
InC	98.9	94	91.31
EKF	99.89	98.9	99.81
Proposed	99.99	99.97	99.96

7. CONCLUSIONS

In this paper, a new method was proposed using a combination of particle and Kalman filters to estimate the irradiation and temperature of a photovoltaic module. Using the estimated values, a new method was applied to the system to track the MPP, which used the power equation derivative, and due to the fact that this method does not require data storage, less memory is used. For evaluation, the proposed method was simulated in three different climatic conditions and compared with the EKF estimation method in terms of estimation accuracy. Also, in these three climatic conditions, the proposed method was compared with EKF and traditional and common InC methods in terms of accuracy and efficiency of MPPT and daily energy generation. The results showed that, firstly, the estimation accuracy of the proposed method is higher than EKF in all the three climatic conditions, and secondly, the proposed method is better than the other two methods in terms of tracking accuracy and efficiency. So, the proposed method is more efficient than EKF method with a rate of 0.1 to 1% and also more efficient than InC method with a rate of 0.8 to 8.65%. In general, it seems that due to the presence of noise in the environment and the measurement sensors, estimation-based methods for tracking perform better than traditional and tracker-based methods and can be a promising candidate for new PV systems.

8. REFERENCES

1. Rupesh, M. and Vishwanath, T., "Intelligent controllers to extract maximum power for 10 kw photovoltaic system", ***International Journal of Engineering, Transactions A: Basics***, Vol. 35, No. 4, (2022), 784-793. https://doi.org/10.5829/ije.2022.35.04A.18
2. Feng, H. and Wang, Y., The application of adaptive algorithm in the maximum power tracking of power photovoltaic system, in Computational and experimental simulations in engineering: Proceedings of icces 2022. 2022, Springer.117-125.
3. Rahimi Mirazizi, H. and Agha Shafiyi, M., "Evaluating technical requirements to achieve maximum power point in photovoltaic powered z-source inverter", ***International Journal of Engineering, Transactions C: Aspects***, Vol. 31, No. 6, (2018), 921-931. https://doi.org/10.5829/ije.2018.31.06c.09
4. Martynyuk, V., Voynarenko, M., Boiko, J. and Svistunov, O., "Simulation of photovoltaic system as a tool of a state's energy security", ***International Journal of Engineering, Transactions B: Applications***, Vol. 34, No. 2, (2021), 487-492. https://doi.org/10.5829/ije.2021.34.02b.21
5. Albatran, S. and Assad, O., "Online adaptive master maximum power point tracking algorithm and sensorless weather estimation", ***Energy Systems***, Vol. 11, (2020), 73-93. https://doi.org/10.1007/s12667-018-0313-9
6. Manna, S., Singh, D.K., Akella, A.K., Abdelaziz, A. and Prasad, M., "A novel robust model reference adaptive mppt controller for photovoltaic systems", ***Scientia Iranica***, (2022). https://doi.org/10.24200/sci.2022.59553.6312
7. Tan, C.W., Green, T.C. and Hernandez-Aramburo, C.A., "An improved maximum power point tracking algorithm with current-mode control for photovoltaic applications", in 2005 International Conference on Power Electronics and Drives Systems, IEEE. Vol. 1, (2005), 489-494.
8. Swaminathan, N., Lakshminarasamma, N. and Cao, Y., "A fixed zone perturb and observe mppt technique for a standalone distributed pv system", ***IEEE Journal of Emerging and Selected Topics in Power Electronics***, Vol. 10, No. 1, (2021), 361-374. https://doi.org/10.1109/JESTPE.2021.3065916
9. Boutabba, T., Drid, S., Chrifi-Alaoui, L. and Benbouzid, M., "A new implementation of maximum power point tracking based on fuzzy logic algorithm for solar photovoltaic system", ***International Journal of Engineering, Transactions A: Basics***, Vol. 31, No. 4, (2018), 580-587. https://doi.org/10.5829/ije.2018.31.04a.09
10. Ishaque, K. and Salam, Z., "A review of maximum power point tracking techniques of pv system for uniform insolation and partial shading condition", ***Renewable and Sustainable Energy Reviews***, Vol. 19, (2013), 475-488. https://doi.org/10.1016/j.rser.2012.11.032
11. Reisi, A.R., Moradi, M.H. and Jamasb, S., "Classification and comparison of maximum power point tracking techniques for photovoltaic system: A review", ***Renewable and Sustainable Energy Reviews***, Vol. 19, (2013), 433-443. https://doi.org/10.1016/j.rser.2012.11.052
12. Motahhir, S., El Hammoumi, A. and El Ghzizal, A., "The most used mppt algorithms: Review and the suitable low-cost embedded board for each algorithm", ***Journal of Cleaner Production***, Vol. 246, (2020), 118983. https://doi.org/10.1016/j.jclepro.2019.118983
13. Lian, K., Jhang, J. and Tian, I., "A maximum power point tracking method based on perturb-and-observe combined with particle swarm optimization", ***IEEE Journal of Photovoltaics***, Vol. 4, No. 2, (2014), 626-633. https://doi.org/10.1109/JPHOTOV.2013.2297513
14. Ghassami, A.A., Sadeghzadeh, S.M. and Soleimani, A., "A high performance maximum power point tracker for pv systems", ***International Journal of Electrical Power & Energy Systems***, Vol. 53, (2013), 237-243. https://doi.org/10.1016/j.ijepes.2013.04.017
15. Boutabba, T., Fatah, A., Sahraoui, H., Khamari, D., Benlaloui, I., Drid, S. and Chrifi-Alaoui, L., "Dspace real-time implementation of maximum power point tracking based on kalman filter structure using photovoltaic system emulator", in 2021 International Conference on Control, Automation and Diagnosis (ICCAD), IEEE., (2021), 1-6.
16. Motahhir, S., Aoune, A., El Ghzizal, A., Sebti, S. and Derouich, A., "Comparison between kalman filter and incremental conductance algorithm for optimizing photovoltaic energy", ***Renewables: Wind, Water, and Solar***, Vol. 4, No. 1, (2017), 8. https://doi.org/10.1186/s40807-017-0046-8
17. Farrokhi, E., Ghoreishy, H., Ahmadiahangar, R. and Rosin, A., "Kalman-filter based maximum power point tracking for a single-stage grid-connected photovoltaic system", in IECON 2021–47th Annual Conference of the IEEE Industrial Electronics Society, IEEE. (2021), 1-6.
18. Abdelsalam, A., Goh, S., Abdelkhalik, O., Ahmed, S. and Massoud, A., "Iterated unscented kalman filter-based maximum power point tracking for photovoltaic applications", in IECON 2013-39th Annual Conference of the IEEE Industrial Electronics Society, IEEE. (2013), 1685-1693.
19. Docimo, D., Ghanaatpishe, M. and Mamun, A., "Extended kalman filtering to estimate temperature and irradiation for maximum power point tracking of a photovoltaic module", ***Energy***, Vol. 120, (2017), 47-57. https://doi.org/10.1016/j.energy.2016.12.089

20. Kumar, N., Singh, B. and Panigrahi, B.K., "Integration of solar pv with low-voltage weak grid system: Using maximize-m kalman filter and self-tuned p&o algorithm", ***IEEE Transactions on Industrial Electronics***, Vol. 66, No. 11, (2019), 9013-9022. https://doi.org/10.1109/TIE.2018.2889617
21. Lefevre, B., Herteleer, B., De Breucker, S. and Driesen, J., "Bayesian inference based mppt for dynamic irradiance conditions", ***Solar Energy***, Vol. 174, (2018), 1153-1162. https://doi.org/10.1016/j.solener.2018.08.090
22. Simon, D., "Optimal state estimation: Kalman, h infinity, and nonlinear approaches, John Wiley & Sons, (2006).
23. Masters, G.M., "Renewable and efficient electric power systems, John Wiley & Sons, (2013).
24. Kayisli, K., "Super twisting sliding mode-type 2 fuzzy mppt control of solar pv system with parameter optimization under variable irradiance conditions", ***Ain Shams Engineering Journal***, Vol. 14, No. 1, (2023), 101950. https://doi.org/10.1016/j.asej.2022.101950
25. Suckow, S., Pletzer, T.M. and Kurz, H., "Fast and reliable calculation of the two-diode model without simplifications", ***Progress in Photovoltaics: Research and Applications***, Vol. 22, No. 4, (2014), 494-501. https://doi.org/10.1002/pip.2301
26. Shannan, N.M.A.A., Yahaya, N.Z. and Singh, B., "Single-diode model and two-diode model of pv modules: A comparison", in 2013 IEEE international conference on control system, computing and engineering, IEEE., (2013), 210-214.
27. Villalva, M.G., Gazoli, J.R. and Ruppert Filho, E., "Modeling and circuit-based simulation of photovoltaic arrays", in 2009 Brazilian Power Electronics Conference, IEEE., (2009), 1244-1254.
28. Jadli, U., Thakur, P. and Shukla, R.D., "A new parameter estimation method of solar photovoltaic", ***IEEE Journal of Photovoltaics***, Vol. 8, No. 1, (2017), 239-247. doi: 10.1109/JPHOTOV.2017.2767602.
29. Jones, A. and Underwood, C., "A thermal model for photovoltaic systems", ***Solar Energy***, Vol. 70, No. 4, (2001), 349-359. https://doi.org/10.1016/S0038-092X(00)00149-3
30. Mattei, M., Notton, G., Cristofari, C., Muselli, M. and Poggi, P., "Calculation of the polycrystalline pv module temperature using a simple method of energy balance", ***Renewable Energy***, Vol. 31, No. 4, (2006), 553-567. https://doi.org/10.1016/j.renene.2005.03.010
31. Abdelhameed, M.M., Abdelaziz, M. and Bayoumi, A., "Enhancement of the output power generated from a hybrid solar thermal system", ***International Journal of Research in Engineering and Technology***, Vol. 3, No. 1, (2014), 322-334.
32. Hartikainen, J., Solin, A. and Särkkä, S., "Optimal filtering with kalman filters and smoothers", Department of biomedica engineering and computational sciences, Aalto University School of Science, 16th August, (2011).
33. Sharifian, M.S., Rahimi, A. and Pariz, N., "Classifying the weights of particle filters in nonlinear systems", ***Communications in Nonlinear Science and Numerical Simulation***, Vol. 31, No. 1-3, (2016), 69-75. https://doi.org/10.1016/j.cnsns.2015.05.021
34. Lee, D.-J., "Nonlinear bayesian filtering with applications to estimation and navigation, Texas A&M University, (2005).

Persian Abstract

چکیده

در این مقاله، روش جدیدی برای ردیابی نقطه حداکثر توان (MPPT) در سیستم‌های فتوولتائیک بر اساس تخمین مقادیر تابش و دما پیشنهاد شده است. روش تخمین پیشنهادی بر اساس ترکیب فیلترهای ذره‌ای و کالمن توسعه‌یافته (EKPF) است. با توجه به اینکه مبنای روش پیشنهادی فیلتر ذره‌ای است، اولاً تخمین با دقت بالایی انجام می‌شود، اگرچه سیستم هدف شدیدا غیر خطی است، ثانیاً محدودیتی برای توابع چگالی احتمال اندازه‌گیری و نویز فرآیند وجود ندارد. این روش برای نویزهای گاوسی و غیر گاوسی کار می کند. برای نشان دادن دقت تخمین، روش پیشنهادی با روش رایج مبتنی بر فیلتر کالمن توسعه یافته (EKF) مقایسه شده و هر دو روش با معیار ریشه میانگین مربعات خطا ارزیابی خواهند شد. با توجه به برآورد دقیق، MPPT با عملکرد خوبی انجام می شود. برای اعتبارسنجی، روش پیشنهادی با روش EKF و روش رایج InC مقایسه می‌شود. شبیه سازی ها نشان می دهد که راندمان از ۰.۱ تا ۱ درصد در مقایسه با EKF و از ۰.۸ تا ۸.۶۵ درصد در مقایسه با روش InC بهبود یافته است که عملکرد روش MPPT پیشنهادی را در محیط های با نویز بالا نشان می دهد.